Catal Lett (2012) 142:1082–1088
DOI 10.1007/s10562-012-0860-y

Comparative Activity of Ni–W and Co–Mo Sulfides Using Transition Metal Oxides as Precursors in HDS Reaction of DBT

Juan Manuel Quintana-Melgoza · Gabriel Alonso-Nuñez · Donald Homero-Galván · Miguel Ávalos-Borja

Received: 15 February 2012 / Accepted: 13 June 2012 / Published online: 6 July 2012

Abstract Unsupported catalysts based on nickel, cobalt, tungsten, and molybdenum were prepared by sulphurization of Ni, Co, W, and Mo oxides. All catalysts were tested in hydrodesulphurization of dibenzothiophene reaction. The best activity was attained with a sample based on W (5.64×10^{16} molecules/s m^2). The best selectivity for biphenyl (70.14 %) was achieved with $Ni_{17}S_{18}$. Materials were characterized by X-ray diffraction and surface area measurements.

Keywords Sulfides · Oxides · HDS · DBT

1 Introduction

Sulphur is present in crude oils in amounts varying from 0.5×10^3 to 50×10^3 ppm, and if present in fuels leads to the formation of sulphur oxides (SO_x), i.e. a form of air pollution generated by internal combustion engines. The environmental regulations to decrease emissions of sulphur and sulphur-containing compounds into the atmosphere have prompted the need to study the process of hydrodesulphurization (HDS) in petroleum feedstocks. The governments of The United States of America, Japan, and Western Europe have restricted the sulphur content of gasoline and diesel fuels from 30 to 50 ppm in 2005 and to less than 10 ppm in 2009–2011 [1–3]. Sulfur compounds can be classified according to the HDS reactivities that are described by the pseudo-first-order rate constant. For example, benzothiophenes are more reactive than dibenzothiophenes (DBTs) but alkyl substituents in positions 4 and 6 in DBT are less reactive in sulfur elimination [4].

Transition metal sulfides (TMS) are widely used as catalysts (generally molybdenum or tungsten sulfides supported on alumina with Co or Ni promoters) designed to remove sulphur bonded to hydrocarbons in the fractions of petroleum formed by cracking processes in refineries [5]. Active sulfide catalysts are prepared by converting oxides to sulfides in a reductive atmosphere such as with hydrogen sulfide [6]. Precursors in hydro-treating catalysts are usually MoO_3 and WO_3 to form MoS_2 and WS_2. The catalytic activity of these disulfides is often enhanced with cobalt or nickel for the HDS reaction [7–9]. Ni–W sulfide catalysts have not been used as frequently as Co–Mo and Ni–Mo sulfide catalysts in hydro-treatments, because W-based catalysts are difficult to convert to sulfides and also because they are less active than Mo-based catalysts in the bulk HDS of gas oil [10]. However, the W-based catalysts are an interesting option in processes where a high hydrogenation potential is required with molecules of high aromatic saturation for oil hydrocracking of intermediate distillates, for the upgrading of coal-derived oils [11], for hydrodenitrogenation (HDN), and for appreciable HDS of diesel fuels [12].

It is well known that hydrogenation catalysts contain different types of active sites that are active for hydrogenolysis and/or hydrogenation, respectively [6]. It is also known that the selectivity or ratio between the two types of

Miguel Ávalos-Borja—On leave at IPICyT, División de Materiales Avanzados, San Luis Potosí, S.L.P., México.

J. M. Quintana-Melgoza
Facultad de Ciencias Químicas e Ingeniería, UABC, Calzada Tecnológico No. 14418, Mesa de Otay, Unidad Universitaria, 22390 Tijuana, B.C., Mexico

G. Alonso-Nuñez · D. Homero-Galván · M. Ávalos-Borja (✉)
Centro de Nanociencias y Nanotecnología (CNyN)-UNAM, Apdo.Postal 2681, 22800 Ensenada, B.C., Mexico
e-mail: miguel_avalos_mx@yahoo.com.mx; miguel@cnyn.unam.mx; miguel.avalos@ipicyt.edu.mx

active sites can be tuned. This selectivity depends on the type of promoter metal (Co or Ni), preparation conditions, and support properties [13]. In a recent study [14], it was shown that Co as a promoter strongly enhances the stacking of MoS_2 layers. However, this effect could be reversed by modifying HDS conditions (pressure, temperature, the ambient atmosphere, etc.) leading then to the formation of single MoS_2 slabs, the presence of which suggests that the majority of active sites on MoS_2 layers are "rim" sites able to perform both hydrogenation and C–S bond cleavage. Co promotion enhances strongly the quality of sites involved in C–S bond cleavage [15]. The number of the active sites in MoS_2, depends on the activation procedure too, as recently shown by Alonso-Núñez et al. [16]. They compared the classical H_2/H_2S atmosphere, with a new N_2/H_2 atmosphere and obtained better stabilized Co/MoS_2 nanoparticles for which Co segregation under the HDS condition is limited. Moreover, depending on the atmosphere used, the activation temperature influences differently the active phase morphology, leading to a rapid sintering at high temperature under N_2/H_2, while the influence is only slightly significant under H_2/H_2S.

The aim of this work is to synthesize sulfides of nickel, tungsten, nickel–tungsten, cobalt, molybdenum, and cobalt–molybdenum, starting with transition metal oxides and not with traditional transition metal salts as precursors for potential catalysts, and then to test them as catalysts in the HDS process with DBT. In addition, the catalytic activity of this group of materials will be compared as a function of their respective transition metal content.

2 Experimental

2.1 Preparation of Catalysts

Cobalt oxide (Co_3O_4) and molybdenum oxide (MoO_3) were obtained from calcinations of cobalt nitrate hydrate $Co(NO_3)_2{\cdot}6H_2O$ (Aldrich Chemical), and ammonium molybdate hydrate $(NH_4)_6Mo_7O_{24}{\cdot}4H_2O$ (Fluka Chemical), at 600 and 500 °C, respectively, for 1 h under an oxygen flow of 1.2 L/h. Bimetallic oxide Co–Mo–O_x (x = 3, 4) was synthesized from a stoichiometric mixture of $(NH_4)_6Mo_7O_{24}{\cdot}4H_2O$ and $Co(NO_3)_2{\cdot}6H_2O$ in a stream of oxygen (1.2 L/h) at 630 °C for 1 h. Nickel oxide (NiO), tungsten oxide (WO_3), and nickel tungstate ($NiWO_4$) were synthesized as previously reported [17], under reaction conditions similar to those used to prepare Co_3O_4, MoO_3, and Co–Mo–O_x (x = 3, 4) which are presented herein. The sulfide catalysts, based on Ni, Co, W, and Mo, were prepared by heating at a rate of 4 °C/min from room temperature to 400 °C under a flow of gaseous H_2/H_2S (15 % H_2S v/v). The temperature was maintained at 400 °C for 4 h for NiO and Co_3O_4 in separate reactions, and for 7 h for the oxides of tungsten and molybdenum, respectively. The oxides used as precursors are NiO, WO_3, $NiWO_4$, Co_3O_4, MoO_3, and Co–Mo–O_x (x = 3, 4). The subsequently obtained catalytic materials are designated as Ni, W, NiW, Co, Mo, and CoMo, respectively.

2.2 X-Ray Diffraction and Surface Area Characterizations

The sulfides were characterized by X-ray diffraction (XRD), and surface area measurements using a Quantachrome Nova 1000 series to determine nitrogen adsorption at −196 °C by the BET method [18]. Samples were degassed under vacuum at 250 °C before nitrogen adsorption measurements. XRD studies were performed using a Philips X Pert MPD diffractometer equipped with a curved graphite monochromator using Cu Kα radiation ($\lambda = 1.54056$ Å) operating at 45 kV and 30 mA. The assignment of the various crystalline phases was based on comparisons with the JCPDS-ICDD powder diffraction file cards [19]. NiO, WO_3 and $NiWO_4$, used as precursors for Ni, W, and NiW catalysts, respectively, were characterized in previous work, also by XRD, scanning electron microscopy (SEM), and surface area measurements [17]. The oxides Co_3O_4, MoO_3, and Co–Mo–O_x (x = 3, 4) and sulfide catalysts of Co, Mo, and CoMo were studied by XRD and surface area measurements.

2.3 Activity of Catalysts

HDS of DBT was carried out in a Parr Model 4520 high-pressure batch reactor (volume: 1 L). The activated catalyst (1.0 g) was placed in the reactor separately. The reactant mixture (6.6 g of DBT in 150 mL of decaline; $[DBT]_0 = 0.239$ mol/L) was added to the autoclave and then pressurized with hydrogen to 3.378 MPa and heated to 350 °C at a rate of 10 °C/min. Once 350 °C was attained, the catalytic reaction was observed for 5 h by analyzing samples using a Perkin Elmer AutoSystem XL gas chromatography equipped with an OV-17 packed column. After the DBT reaction was complete, the catalysts were filtered, washed with isopropanol to remove residual hydrocarbons, and dried at room temperature as ascertained by surface measurements.

3 Results and Discussion

Figures 1, 2, 3, 4 show XRD patterns in which the observed intensities are labeled with the corresponding Miller index (*hkl*) notation for catalysts Ni, W, NiW, Co, Mo, CoMo, and their precursors Co_3O_4, MoO_3, Co–Mo–O_x (x = 3, 4) of the last three catalysts, before HDS reaction.

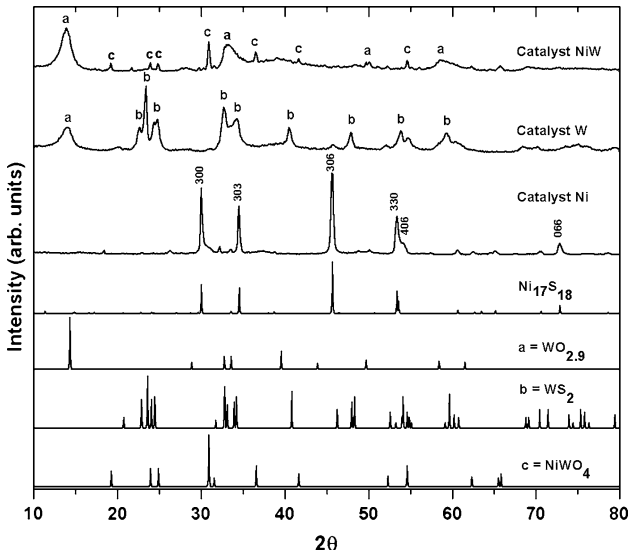

Fig. 1 Experimental XRD patterns corresponding to catalyst Ni, W, and NiW, and XRD simulations (from JCPDS-ICDD files) for $Ni_{17}S_{18}$ (76-2306). *a* $WO_{2.9}$ (05-0386); *b* WS_2 (08-0237); *c* $NiWO_4$ (15-0755)

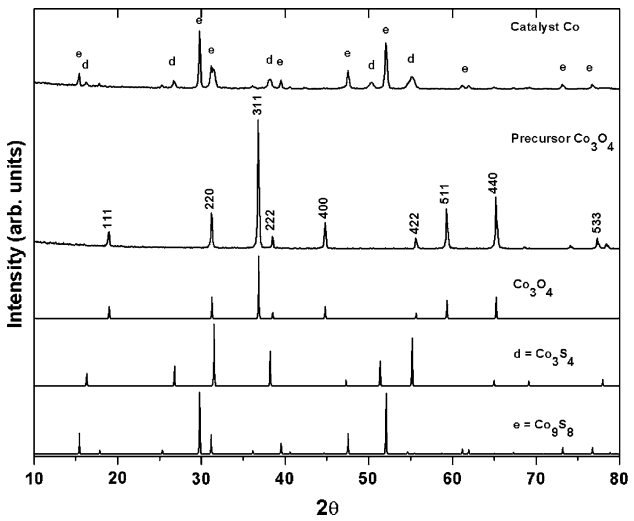

Fig. 2 Experimental XRD patterns corresponding to catalyst Co, and Co_3O_4 used as precursor for catalyst Co, and XRD simulations (from JCPDS-ICDD files) for Co_3O_4 (42-1467), *d* Co_3S_4 (73-1703); *e* Co_9S_8 (65-6801)

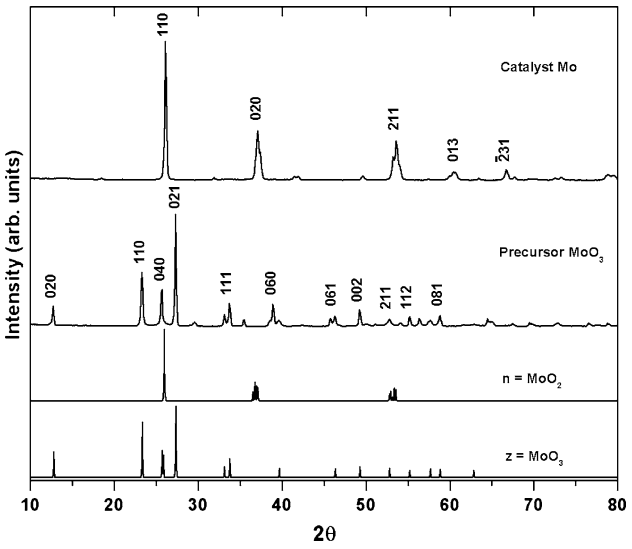

Fig. 3 Experimental XRD patterns corresponding to catalyst Mo, and MoO_3 used as precursor for catalyst Mo, and XRD simulations (from JCPDS-ICDD files) for *n* MoO_2 (78-1073); *z* MoO_3 (35-0609)

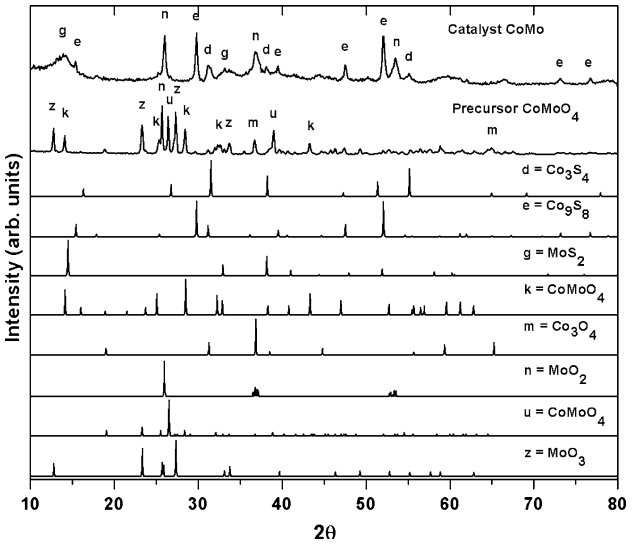

Fig. 4 Experimental XRD patterns corresponding to catalyst CoMo and its precursor $CoMoO_4$, and XRD simulations (from JCPDS-ICDD files) for *d* Co_3S_4 (73-1703); *e* Co_9S_8 (65-6801); *g* MoS_2 (74-0932); *k* $CoMoO_4$ (25-1434); *m* $Co3O_4$ (42-1467); *n* MoO_2 (78-1073); *u* $CoMoO_4$ (21-0868); *z* MoO_3 (35-0609)

If an XRD pattern contains more than one phase, it is denoted by a lower case letter. The ratio of the crystallographic phases which constitute each catalyst was estimated from the area under the curve for the main peak in the diffractogram (*hkl* columns in Table 1). The diffractogram (Fig. 1) of the Ni catalyst is indicative of the pure $Ni_{17}S_{18}$ phase. Catalyst W (Fig. 1) consists of two phases: tungsten sulfide WS_2 (label "a" in Fig. 1) (57 wt% or w/o) and tungsten oxide $WO_{2.9}$ (label "b" in Fig. 1) (43 w/o). The NiW catalyst is composed of 11 w/o $NiWO_4$ (label "c" in Fig. 1) and 89 w/o WS_2 (label "a" in Fig. 1). The phases identified as $Ni_{17}S_{18}$, WS_2, $WO_{2.9}$, and $NiWO_4$ are in agreement with JCPDS-ICDD card numbers 76-2306, 08-0237, 05-0386, and 15-0755, respectively [19] (for brevity, subsequent references to the abbreviation for this database will be omitted and only the card numbers like 15-0755, for example, will be cited).

Figure 2 shows two diffractograms: the first pattern confirms the pure crystalline phase of Co_3O_4 (42-1467), used as a precursor of the Co catalyst in this work, and the second pattern shows two crystalline phases of cobalt

Table 1 Average crystal size of maximum diffraction peak (*hkl*) by Debye–Scherrer analysis (C_{XRD}), ratio of crystallographic phases, and surface area by BET method (S_{BET}), for all the catalysts and oxides precursors

Catalyst	Phases of catalyst	C_{XRD} (Å)	Selected X-ray peaks (*hkl*)	Phase ratio	S_{BET} (m^2/g)	Precursor	C_{XRD} (Å)	Selected X-ray peaks (*hkl*)	Phase ratio	S_{BET} (m^2/g)
Ni	$Ni_{17}S_{18}$	796	306	1.0	6.3	NiO	870	012	1.0	3.0
W	WS_2	127	002	0.57	6.4	WO_3	1,010	200	1.0	2.0
	$WO_{2.9}$	606	010	0.43						
NiW	WS_2	126	002	0.89	9.9	$NiWO_4$	1,020	$\bar{1}11$	1.0	11
	$NiWO_4$	826	$\bar{1}11$	0.11						
Co	Co_9S_8	1,022	311	0.54	3.1	Co_3O_4	1,312	311	1.0	3.2
	Co_3S_4	409	311	0.46						
Mo	MoO_2	940	110	1.0	12.0	MoO_3	1,211	021	1.0	5.0
CoMo	MoS_2	116	003	0.28	5.0	$CoMoO_4$	1,026	002	0.26	3.5
	MoO_2	679	110	0.25		CoO–MoO_3	888	220	0.21	
	Co_9S_8	807	311	0.26		MoO_3	1,019	020	0.36	
	Co_3S_4	271	311	0.21		Co_3O_4	751	311	0.17	

sulfide that make up the Co catalysts: 46 w/o Co_3S_4 (label d) and 54 w/o Co_9S_8 (label e) (73-1703 and 65-6801, respectively).

Figure 3 represents two XRD patterns which correspond to catalyst Mo and its precursor. In this case, the oxide used as precursor of catalyst Mo is in agreement with the MoO_3 phase, (35-0609). Catalyst Mo is identified as 100 % of the MoO_2 phase (78-1073). Even at the longest reaction time of 7 h, this reaction leads to the formation of MoO_2 instead of the desired MoS_2, which indicates that the replacement of oxygen by sulfur does not occur under the time–temperature conditions examined here, in spite of the presence of excess sulfur. Furthermore, the Mo–O bonds of MoO_3 are known to have less ionic character than those in WO_3 [20], similar to experimental results obtained with WS_2 and MoO_2.

In Fig. 4, two distinct patterns are evident from XRD analysis of catalyst CoMo and its precursor, Co–Mo–O_x ($x = 3, 4$). Catalyst CoMo is composed of the following crystalline phases: 28 w/o MoS_2 (label g), 25 w/o MoO_2 (label n), 26 w/o Co_9S_8 (label e), and 21 w/o Co_3S_4 (label d), (74-0932, 78-1073, 65-6801, and 73-1703, respectively). The precursor of catalyst CoMo contains a mixture of oxides, identified as 21 w/o $CoMoO_4$ (label k), 26 w/o CoO–MoO_3 (label u), 36 w/o MoO_3 (label z), and 17 w/o Co_3O_4 (label m), (25-1434, 21-0868, 35-0609, and 42-1467, respectively). Table 1 lists the ratios of the crystallographic phases of oxides and catalysts observed in this work.

The surface areas of catalysts and oxides are shown in Table 1. The catalysts Ni, W, and Mo have surface areas which are greater than those of the corresponding precursor oxides, i.e. twice as much for catalyst Ni compared to NiO (from 3.0 to 6.3) m^2/g, three times as much for catalyst W compared to WO_3 (from 2.0 to 6.4) m^2/g, and twice as much for catalyst Mo compared to MoO_3 (from 5.0 to 12.0) m^2/g. Nevertheless, in the catalysts NiW, Co, and CoMo major changes in surface area are not observed compared to the corresponding oxides. These values are 9.9, 3.1, and 5.0 m^2/g, respectively, compared to 11, 3.2, and 3.5 m^2/g. The surface areas of catalysts, in decreasing order, are shown in Table 1: Mo > NiW > W > Ni > CoMo > Co. Pore size for all catalysts is in the range of 17–159 Å and the corresponding pore volume is in the range 5.6×10^{-2} to 5.7×10^{-3} cm^3/g [21]. The catalysts show the following decreasing order of pore volume: NiW > Mo > W > CoMo > Ni > Co, which is the same trend as the surface area for these catalysts. In this case, the nitrogen adsorption–desorption curves correspond to isotherm type IV (Fig. 5), with characteristic desorption curves of mesoporous

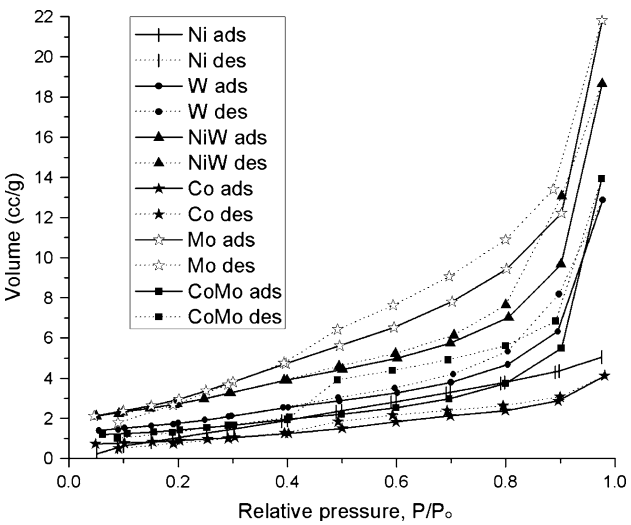

Fig. 5 Nitrogen adsorption (ads)–desorption (des) *curves* corresponding to isotherms of Ni, W, NiW, Co, Mo, and CoMo catalysts

materials [22], in agreement with the pore size diameter in the range of 20–500 Å, reported by Leofanti et al. [23]. Precision in the determination of surface area is estimated to be ±3 %, based on experimental error.

DBT conversion as a function of time at constant temperature of 350 °C for all the catalysts is shown in Fig. 6. The rate constant (k specific) was calculated by assuming DBT conversion to be pseudo-zero order reaction according to the equation: $X_{DBT} = (1-\eta_{DBT}/\eta_{DBT}) = (k/\eta_{DBT,0})t$, where X_{DBT} is the fractional conversion of DBT, η_{DBT} = moles of DBT, k = pseudo-zero order rate constant, t = time in seconds and $(k/\eta_{DBT,0})$ = the slope [24]. The catalytic activity (k specific) range from 1.42×10^{-7} to 8.91×10^{-7} mol/(s g) and the main reaction products are biphenyl (BP) and cyclohexyl-benzene (CHB). However, in order to compare with other results in the literature, we have changed the units of k specific to molecules/(s m^2) [25]. (This is achieved by multiplying the activity (mol/(s g)) by Avogadro's number (6.022×10^{23} molecules/mol) and dividing by the surface area (m^2/g)). The values of k specific (in these units), range from 1.37×10^{16} to 5.64×10^{16} molecules/(s m^2) according to the following order of catalysts: W > NiW > Ni > CoMo > Co > Mo. The values of catalytic activity for the catalysts synthesized in this work are summarized in Table 2. We also present in Table 3 k specific values from the literature [3, 6, 9, 25–30]. As seen, the activities shown in Table 3 are similar to the activities of our catalysts presented in Table 2.

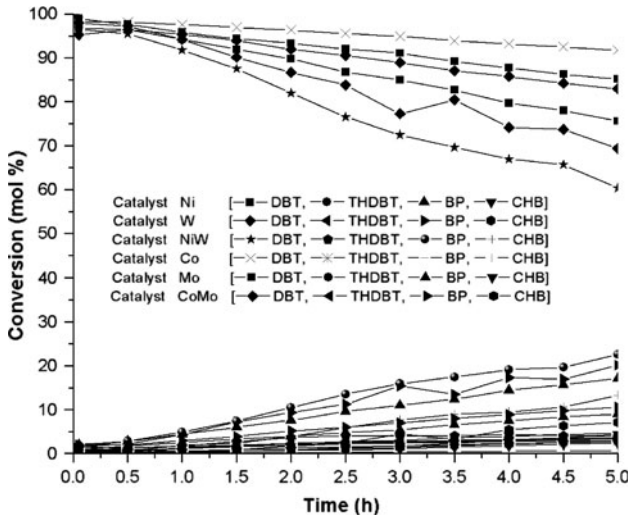

Fig. 6 The reaction of HDS with DBT in the presence of catalysts Ni, W, NiW, Co, Mo, or CoMo, including the tetrahydrodibenzothiophene intermediate (THDBT) and the products: BP and CHB

As shown in Fig. 7, BP is formed by hydrogenation of one π bond of one of the aromatic rings of DBT, in which dihydrodibenzothiophene (DHDBT) is produced as an intermediary, followed by C–S bond cleavage and reformation of the aromatic ring of DBT (direct desulphurization pathway: DDS). In comparison, CHB is produced by hydrogenation of two π bonds followed at equilibrium by hydrogenation of a third π bond of one aromatic ring of DBT to form two intermediaries, the THDBT and hexahydrodibenzothiophene (HHDBT), followed by C–S bond rupture (hydrogenation pathway: HYD) [9], as shown in Fig. 7 also. In this reaction, neither bicyclohexyl nor benzene is formed.

Selectivity was determined for main reaction products BP and CHB. Since DDS and HYD are parallel pathways [31], the ratio between both pathways can be approximated in terms of experimental selectivity from the equation: HYD/DDS = CHB/BP. Selectivity is found in the range

Table 3 Reaction rate coefficient (k specific) reported in the literature for some catalysts in HDS reaction

Catalyst	k specific (molecules/s m^2)	Reference
$Co/MoS_{2\ ex\ situ}$	3.13×10^{16}	[3]
WS_2	4.12×10^{15}	[6]
$Ni/ATT_{\ in\ situ}$	5.19×10^{16}	[9]
Ni_3S_2/MoS_2	4.01×10^{16}	[25]
$Ni/H–WS_{2\ in\ situ}$	5.12×10^{16}	[26]
MoS_2	6.37×10^{14}	[27]
Co12	8.22×10^{15}	[28]
$Co/MoS_2/Al_2O_3$ (CCat)	2.48×10^{15}	[28]
$CoMo–C_4$	4.12×10^{15}	[29]
$Ni–Mo–W_{\ ex\ situ}$	2.61×10^{16}	[30]
$NiMo/Al_2O_3$ (Ind)	4.41×10^{15}	[30]

CCat commercial catalyst, *Ind* industrial catalyst

Table 2 Surface area of sulfides and oxides, reaction rate coefficient (k specific), products of reaction: THDBT, CHB, BP, and selectivity (CHB/BP) for all the catalysts

Catalyst	Sulfides (m^2/g)	Oxides (m^2/g)	k specific × 10^{-7} (mol/s g)	k specific × 10^{16} (molecules/s m^2)	THDBT (%)	CHB/BP (% ratio)
Ni	6.3	3.0	4.61	4.40	12.03	17.83/70.14 = 0.25
W	6.4	2.0	6.00	5.64	10.98	23.13/65.89 = 0.35
NiW	9.9	11.0	8.91	5.42	9.55	33.52/56.93 = 0.59
Co	3.1	3.2	1.42	2.76	33.51	9.12/57.36 = 0.16
Mo	12.0	4.9	2.74	1.37	22.99	16.08/60.92 = 0.26
CoMo	5.0	3.5	3.07	3.69	20.84	17.22/61.94 = 0.28

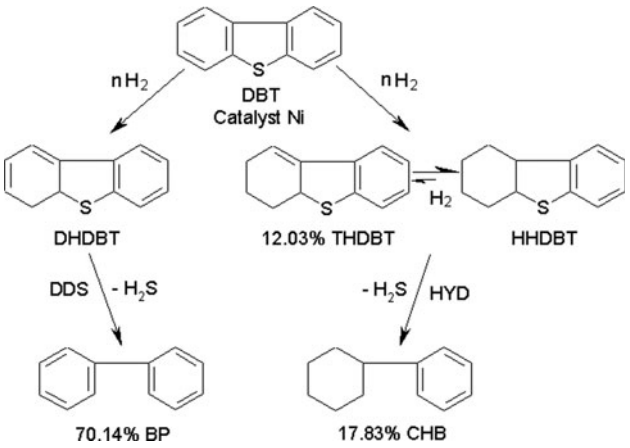

Fig. 7 Reaction network for the HDS of DBT by direct desulphurization pathway (DDS) and the hydrogenating pathway (HYD) to produce BP and CHB. nH_2 = excess gaseous hydrogen at 3.378 MPa, DHDBT, THDBT, HHDBT, H_2S = hydrogen sulphide. The percentages of products THDBT (12.03 %), CHB (17.83 %), and BP (70.14 %) are normalized to the percentages obtained with the Ni catalyst

from 0.16–0.59 (CHB/BP ratio in Table 2) for the following catalysts: Co < Ni < Mo < CoMo < W < NiW. As can be seen in Table 2, all catalysts have selectivity for BP with HYD/DDS < 1 via the DDS route. In addition, as shown in Table 2, BP is produced in yields of 56.93–70.14 % for the following decreasing order of catalytic activity: Ni > W > CoMo > Mo > Co > NiW. The activity of unsupported monometallic TMS for HDS of DBT has been reported by Pecoraro and Chianelli [32] as volcano plots, with the maximum value occurring for Ru and Os. However, the periodic tendency for TMS is Ru > Os > Rh ≈ Ir > Re > Pt > Pd > Mo > Cr > W > Nb ≈ Sn > Ni ≈ Au > Co ≈ Ti > Fe ≈ V ≈ Zr ≈ Ta > Mn [32]. The percentage of 4d or 5d electronic character in Ru, Rh, Ir and Os are as high as 50 %, in accordance with % d-character suggested by Pauling [33]. This reflects a high degree of covalent bond character, which is an important property of heterogeneous catalytic materials with high activity in HDS [34]. In this work, catalysts Ni, W, NiW, Co, Mo, and CoMo contained transition metals Ni, W, Co, and Mo. According to Pecoraro and Chianelli, the expected activity for these metals is in descending order: Mo > W > Ni > Co.

Crystallographic phases of the catalysts Ni, W, NiW, Co, Mo, and CoMo have shown DBT HDS catalytic activity consistent with the formation of TMS. In the case of catalyst W, the ratio of $WS_2/WO_{2.9} = 1.32$ which may account for its high activity. In catalyst NiW, the ratio $WS_2/NiWO_4 = 8$ and its high content of WS_2 may account for more activity than the catalyst W itself. However, the presence of $NiWO_4$ may decrease its activity. In order of activity, the catalyst Ni ($Ni_{17}S_{18}$) is less active than catalysts W and NiW in terms of TMS production. Nevertheless, this phase is the most selective to BP formation, perhaps because of the electronic properties of nickel, as reported by Mangnus et al. [8]. Catalyst Mo is the least active of the six catalysts studied here, perhaps because it is an oxide (MoO_2), which has been shown to be less active than the catalyst Co, formed from cobalt sulfides (Co_9S_8, Co_3S_4), and also much less active than catalyst CoMo, which contains MoS_2 (0.28 w/o), see the Tables 1 and 2.

4 Conclusions

The synthetic method presented here appears to be an alternative way of preparing the TMS of Ni, Co, and W with high catalytic activity and selectivity in HDS of DBT. Catalyst W with a composition of 57 wt % WS_2 and 43 w/o $WO_{2.9}$ is the most active for the HDS reaction with a rate of 5.64×10^{16} molecules/(s m^2) for DBT conversion to BP (yield = 65.89 %), CHB (yield = 23.13 %) and THDBT (yield = 10.98 %). The bimetallic precursor Ni–W is easier to convert to the corresponding sulfide than the bimetallic precursor Co–Mo. This can be seen with the catalysts NiW and CoMo, in which the former was obtained from Ni–W at a WS_2 ratio of 0.89 and the latter was obtained from Co–Mo in MoS_2 with a ratio of 0.28. Furthermore, conversion of MoO_3 to MoS_2 is not achieved at 400 °C and instead results in the formation of MoO_2. Selectivity of all catalysts favored the formation of BP over CHB with catalyst Ni ($Ni_{17}S_{18}$ phase) being the most selective to BP formation (yield = 70.14 %). According to the results shown herein, it appears that the $Ni_{17}S_{18}$ phase may be a new material for use in HDS catalysts.

Acknowledgments The authors acknowledge financial support from PROMEP/103.5/03/1101, DGAPA-UNAM (grant IN-108908) and Conacyt (grant 2010-151551). We are very grateful to E. Aparicio, F. Ruiz, E. Flores, I. Gradilla, M. Sainz, J. Peralta, C. Ornelas and P. Riley (Peace Corps/Mexico) for technical assistance.

References

1. Funamoto T, Segawa K (2005) Proceedings of 15th Saudi–Japan joint symposium, Dhahran, pp 1–10
2. Iwamoto M, Hamada H (1991) Catal Today 10:57–71
3. Alvarez L, Espino J, Ornelas C, Rico JL, Cortez MT, Berhault G, Alonso G (2004) J Mol Catal A Chem 210:105–117
4. Pawelec et al (2011) Catal Sci Technol 1:23–42
5. Chianelli et al (2009) Catal Today 147:275–286
6. Alonso G, Chianelli RR (2004) J Catal 221:657–661
7. Ramanathan K, Weller SW (1985) J Catal 95:249–259
8. Mangnus PJ, Bos A, Moulijn JA (1994) J Catal 146:437–448
9. Espino J, Alvarez L, Ornelas C, Rico JL, Fuentes S, Berhault G, Alonso G (2003) Catal Lett 90:71–80
10. Reinhoudt HR, Van Langeveld AD, Kooyman PJ, Stockmann RM, Prins R, Zandbergen HW, Moulijn JA (1998) J Catal 179:443–450

11. Yoshimura Y, Sato T, Shimada H, Matsubayashi N, Imamura M, Nishijima A, Higo M, Yoshitomi S (1996) Catal Today 29:221–228
12. Woo SI, Kim CH, Yoon WL, Lee IC (1996) Appl Catal A Gen 144:159–175
13. Leliveld RG et al (2008) Catal Today 130:183–189
14. Berhault G, de la Rosa MP, Mehta A, Vacaman MJ, Chianelli RR (2008) Appl Catal A Gen. 345:80–88
15. Stanislaus A et al (2010) Catal Today 153:1–68
16. Alonso-Núñez G, Bocarando J, Huirache-Acuña R, Álvarez-Contreras L, Huang Z-D, Bensch W, Berhault G, Cruz J, Zepeda TA, Fuentes S (2012) Appl Catal A 419–420:95–101
17. Melgoza JMQ, Cortés AG, Avalos-Borja M (2002) React Kinet Catal Lett 76:131–140
18. Brunauer S, Emmett PH, Teller E (1938) J Am Chem Soc. 60:309–319
19. Joint Committee on Powder Diffraction Standards (JCPDS)-International Centre for Diffraction Data (ICDD) (2010)
20. Kung HH (1989) Transition Metal Oxides: Surface Chemistry and Catalysis, 1st edn. Elsevier Science Publishers B.V, New York, p 32
21. Barrett EP, Joyner LG, Halenda PP (1951) J Am Chem Soc 73:373–380
22. Ciobanu CS, Andronescu E, Predoi D (2011) Dig J Nanomater Biostruct 6(3):1239–1244
23. Leofanti G, Padovan M, Tozzola G, Venturelli B (1998) Catal Today 41:207–219
24. Olivas A, Alonso G, Fuentes S (2006) Top Catal 39:175–179
25. Harris S, Chianelli RR (1986) J Catal 98:17–31
26. Alonso G, Espino J, Berhault G, Alvarez L, Rico JL (2004) Appl Catal A Gen 266:29–40
27. Alonso G, Siadati MH, Berhault G, Aguilar A, Fuentes S, Chianelli RR (2004) Appl Catal A Gen. 263:109–117
28. Rivera-Muñoz E, Alonso G, Siadati MH, Chianelli RR (2004) Catal Lett 94:199–204
29. Nava H, Ornelas C, Aguilar A, Berhault G, Fuentes S, Alonso G (2004) Catal Lett 86:257–265
30. Olivas A, Galvan DH, Alonso G, Fuentes S (2009) Appl Catal A 352:10–16
31. Whitehurst DD, Isoda T, Mochida I (1998) Adv Catal 42:345–471
32. Pecoraro TA, Chianelli RR (1981) J Catal 67:430–445
33. Pauling L (2001) Selected Scientific Papers 20th century chemistry. In: Kamb B et al (ed) World Scientific series vol 10.vol 1, pp 384–385
34. Chianelli RR, IFP (Institut français du pétrole) (2006) Oil Gas Sci Technol Rev 61:503–513